

# Gas-Generating Porous Electrodes at Low Overvoltages: Allowance for the Outside-Electrode Limitations

Yu. G. Chirkov

Frumkin Institute of Electrochemistry, Russian Academy of Sciences, Leninskii pr. 31, Moscow, 117071 Russia

Received April 12, 1999; in final form, July 9, 1999

**Abstract**—Characteristics of gas-generating porous electrodes (GPE) are calculated and analyzed at low overvoltages, when all the electrode pores are still filled with electrolyte. The calculations assume the existence of limitations outside the electrode, specifically, the diffusion of gas molecules dissolved in electrolyte and their conglomeration into bubbles. Separate solutions are found and then sewn for GPE and the electrolyte chamber outside it, where the generated gas is collected. An important parameter is revealed, namely, the ratio of a characteristic gas-generation current inside GPE to a characteristic gas-removal current inside the outside-electrode region. The parameter determines both the net current density in GPE and the depth of the electrochemical process penetration into the electrode's porous space. The two limiting cases studied are the hydrogen-generating water electrolysis on a porous platinum electrode and the chlorine generation on dimensionally stable anodes (DSA). A way to estimate all quantities that characterize the gas removal into the outside-electrode region is shown. It is established that only a narrow (no greater than a micrometer) region adjacent to the front surface of GPE takes part in the chlorine generation process on DSA of standard thickness (5 μm).

## 1. THE POROUS ELECTRODE

Consider the gas-generation process in a porous electrode. The coordinates of this region are  $0 < y < \Delta$ , where  $\Delta$  is the electrode thickness. Suppose that the limiting stage of the electrochemical formation of gas molecules on the surface of pores in a gas-generating porous electrode (GPE) is a slow discharge. Then, the current density  $j$  of discharge is related to a reduced overvoltage  $\eta = FE/RT$  as follows:

$$j = i_0(e^{\beta\eta} - \bar{c}e^{-\alpha\eta}). \quad (1)$$

Here,  $i_0$  is the exchange current of the electrochemical reaction;  $\bar{c} = c/c_0$  is the solution oversaturation with gas;  $c_0$  is the gas solubility; while  $\alpha$  and  $\beta$  are the apparent or true transfer coefficients for cathodic and anodic processes, respectively, depending on which particular process is being considered. The oversaturation distribution over the GPE thickness obeys the equation

$$d^2\bar{c}/d\bar{y}^2 = \bar{c} - e^{(\alpha+\beta)\eta}. \quad (2)$$

Here,  $\bar{y} = y/L_d$  is the reduced coordinate referred to the front side of GPE, and

$$L_d = (nFD^*c_0/Si_0)^{1/2}e^{\alpha\eta/2} = L_d^0e^{\alpha\eta/2} \quad (3)$$

is a characteristic diffusion length of GPE. In (3),  $S$  is the specific surface which sustains the electrochemical reaction and  $D^*$  is the effective diffusion coefficient

$$D^* = Dg_l/v = D_{\max}/v, \quad (4)$$

where  $D$  is the true diffusion coefficient for the gas in electrolyte,  $g_l$  is the liquid porosity, and  $v > 1$  is a physi-

cally meaningless quantity which shows how much  $D$  differs from a maximum possible coefficient  $D_{\max}$  and depends on the porous space structure. The two distinctive types of porous media are modeled as lattices of sites and lattices of bonds [1, 2]. According to some calculations,  $v = 1$  for the former and  $v \gg 1$  for the latter. Equation (2) must be supplemented with two boundary conditions

$$y = 0 \quad \bar{c} = \bar{c}_s \quad y = \Delta \quad d\bar{c}/d\bar{y} = 0, \quad (5)$$

where  $\bar{c}_s$  is the oversaturation on the front surface of GPE. Solving (2) together with (5) yields the oversaturation distribution over the GPE thickness

$$\bar{c} = e^{(\alpha+\beta)\eta} + (\bar{c}_s - e^{(\alpha+\beta)\eta}) \times \cosh[(\Delta - y)e^{-\alpha\eta/2}/L_d^0] / \cosh[\Delta e^{-\alpha\eta/2}/L_d^0]. \quad (6)$$

The oversaturation reaches a maximum near the rear side of GPE. The dependence of  $\bar{c}_\Delta$  on the overvoltage follows from (6), taking  $y = \Delta$ . Then,

$$\bar{c}_\Delta = e^{(\alpha+\beta)\eta} + (\bar{c}_s - e^{(\alpha+\beta)\eta}) / \cosh[\Delta e^{-\alpha\eta/2}/L_d^0]. \quad (7)$$

Expression (6) allows us to determine the reduced net current density (the amount of gas generated in GPE per cm<sup>2</sup> of its front surface) as well:

$$\bar{i} = I/I_d = e^{-\alpha\eta/2}(e^{(\alpha+\beta)\eta} - \bar{c}_s) \tanh(\Delta e^{-\alpha\eta/2}/L_d^0). \quad (8)$$

Here,  $I_d$  is a characteristic diffusion current of a porous electrode

$$I_d = (nFD^*c_0Si_0)^{1/2}. \quad (9)$$

For calculations, we may also need parameter  $\xi$  which characterizes how closely the gas generation mode in a

GPE approaches a kinetic mode in which the amount of generated gas is the largest:

$$I = I_k(e^{\beta\eta} - e^{-\alpha\eta}), \quad (10)$$

where  $I_k$  is the characteristic kinetic current

$$I_k = Si_0\Delta. \quad (11)$$

Parameter  $\xi$  apparently lies between zero and unity. The latter value is typical for a purely kinetic gas-generation mode. The overvoltage dependence of  $\xi$  is described by the expression

$$\xi = I/I_k(e^{\beta\eta} - e^{-\alpha\eta}) = (I_d/I_k) \times [e^{-\alpha\eta/2}(e^{(\alpha+\beta)\eta} - \bar{c}_s) \tanh(\Delta e^{-\alpha\eta/2}/L_d^0)]/(e^{\beta\eta} - e^{-\alpha\eta}). \quad (12)$$

As shown in [3] and review [4], in an electrolyte-filled cylindrical pore of radius  $R$ , once the saturation of electrolyte with gas increased, there comes an instant when critical oversaturation  $\bar{c}^*$  is reached. At such an instant, an equilibrium gas nucleus forms in the pore. Then, the latter completely gets rid of electrolyte and turns a "gas" pore. This condition has the form

$$\bar{c}^* = c^*/c_0 = 1 + r_0/R. \quad (13)$$

Here,  $r_0$  is a characteristic radius of the gas nucleus:  $r_0 = 2\sigma/P_0$ , where  $\sigma$  is the surface tension and  $P_0$  is atmospheric pressure. In normal conditions,  $r_0 = 1 \mu\text{m}$ . Condition (13) allows us to determine the critical overvoltage  $\eta^*$ , at which first gas-filled pores emerge in a GPE. In accordance with (6), a maximum oversaturation occurs in pores of the rear side of GPE, at  $y = \Delta$ . Hence, equating left parts of (7) and (13), i.e., equating  $\bar{c}^*$  and  $\bar{c}_\Delta$ , we obtain the condition that determines the magnitude of  $\eta^*$ :

$$e^{(\alpha+\beta)\eta^*} + (\bar{c}_s - e^{(\alpha+\beta)\eta^*})/\cosh[\Delta e^{-\alpha\eta^*/2}/(nFD^*c_0/Si_0)^{1/2}] = 1 + r_0/R, \quad (14)$$

where  $R$  is now a maximum possible radius of pores in GPE.

## 2. THE ELECTROLYTE CHAMBER

Consider now the mechanism of the gas removal from GPE and processes that occur in the outside-electrode space, i.e. in the electrolyte chamber. Coordinates of this space are  $\infty < y < 0$ . A real electrolyte chamber has finite size, but we assume that its dimensions exceed the characteristic diffusion length of the gas removal process in the chamber. The function of a GPE is to produce a gas product of the electrochemical reaction that proceeds at its inner surface. At low overvoltages, gas molecules that form in GPE are dissolved in electrolyte. They are removed into the electrolyte chamber through diffusion. In the stagnant electrolyte solution (we restricted ourselves to this case only), the

gas generated in GPE converts into the gas product, after a long sequence of successive processes. These involve the formation of gas nuclei and their reaching a critical size, the growth of gas bubbles and their agglomeration, and the flotation and removal of large gas bubbles beyond the electrolyte chamber. It is pretty difficult to account for all these stages, especially in view of the electrolyte chamber design and its geometry. We can only state that the overall flux of conversion of gas molecules dissolved in electrolyte into gas bubbles in a unit volume of electrolyte in a unit time period  $j_g$  is likely to be proportional to the excess of the electrolyte oversaturation with gas over the equilibrium value of this quantity. In other words, we assume that

$$j_g = \psi(\bar{c} - 1), \quad (15)$$

where the constant  $\psi$  is expressed in  $\text{mol cm}^{-3} \text{s}^{-1}$ . Hence, the distribution of the electrolyte oversaturation with gas over the electrolyte chamber thickness is described by the equation

$$d^2\bar{c}/d\bar{y}^2 = \bar{c} - 1. \quad (16)$$

Here,  $\bar{y}$  is a reduced coordinate referred to the front surface of GPE:  $\bar{y} = y/L_g$ , where  $L_g$  is the characteristic diffusion length for the electrolyte chamber

$$L_g = (Dc_0/\psi)^{1/2}. \quad (17)$$

Equation (16) calls for two boundary conditions

$$y = 0 \quad \bar{c} = \bar{c}_s \quad y = -\infty \quad d\bar{c}/d\bar{y} = 0. \quad (18)$$

The latter condition implies that gas molecules dissolved in the electrolyte chamber cannot be removed through diffusion. The gas must agglomerate into gas bubbles and leave the electrolyte chamber only in this form. Solution of equation (16) yields the distribution of the electrolyte oversaturation with gas over the electrolyte chamber thickness

$$\bar{c} = (\bar{c}_s - 1)e^{y/L_g} + 1. \quad (19)$$

Equation (19) leads to a definition for the reduced net current density that differs from (8):

$$\bar{I} = I/I_g = (\bar{c}_s - 1), \quad (20)$$

where  $I_g$  is a characteristic diffusion current for the electrolyte chamber

$$I_g = nFDc_0/L_g = nF(Dc_0\psi)^{1/2}. \quad (21)$$

## 3. SEWING THE SOLUTIONS

Solutions for the diffusion equations in two regions, namely, GPE and electrolyte chamber include parameter  $\bar{c}_s$ , which is the oversaturation at the front surface of GPE and is unknown. To find it, the net current densities in GPE must be equated to those in the electrolyte chamber. Utilizing definitions (8) and (20) and equat-

ing the currents in these expressions, we obtain the ultimate condition for the determination of parameter  $\bar{c}_s$

$$I_d e^{-\alpha\eta/2} (e^{(\alpha+\beta)\eta} - \bar{c}_s) \tanh(\Delta e^{-\alpha\eta/2}/L_d^0) = I_t (\bar{c}_s - 1). \quad (22)$$

Then,

$$\bar{c}_s = [\varphi e^{(\alpha/2+\beta)\eta} \tanh(\Delta e^{-\alpha\eta/2}/L_d^0) + 1] / [\varphi e^{-\alpha\eta/2} \tanh(\Delta e^{-\alpha\eta/2}/L_d^0) + 1], \quad (23)$$

where parameter  $\varphi$  is equal to the ratio between characteristic currents in GPE and electrolyte chamber:

$$\varphi = I_d/I_t = (Si_0 g_l/nF\psi v)^{1/2}. \quad (24)$$

The oversaturation on the front surface of GPE, which is defined by expression (23), may be substituted in either equation for the net current densities, (8) and (20). Hence, the net current density may be described by two equivalent expressions

$$I = I_d e^{-\alpha\eta/2} (e^{(\alpha+\beta)\eta} - [\varphi e^{(\alpha/2+\beta)\eta} \tanh(\Delta e^{-\alpha\eta/2}/L_d^0) + 1] / [\varphi e^{-\alpha\eta/2} \tanh(\Delta e^{-\alpha\eta/2}/L_d^0) + 1]) \tanh(\Delta e^{-\alpha\eta/2}/L_d^0), \quad (25)$$

$$I = I_g ([\varphi e^{(\alpha/2+\beta)\eta} \tanh(\Delta e^{-\alpha\eta/2}/L_d^0) + 1] / [\varphi e^{-\alpha\eta/2} \tanh(\Delta e^{-\alpha\eta/2}/L_d^0) + 1] - 1). \quad (26)$$

Let us enlarge on one feature generic for the gas generation in GPE. In part, we have already discussed this point in [5–7]. For the transfer coefficient  $\alpha \neq 0$ , it seems impossible to introduce the notions “thin” and “thick” electrodes. There is no GPE size that would be independent of the GPE oversaturation and above which the GPE characteristics would stop depending on the GPE thickness. Because, as follows from the net current density definition (25), at any arbitrarily large but fixed GPE thickness, the argument of the hyperbolic tangent  $\tanh(\Delta e^{-\alpha\eta/2}/L_d^0)$  becomes small with increasing the overvoltage, and the net current density begins to linearly rise with increasing GPE thickness. The division into thin and thick electrodes is relevant only when the transfer coefficient vanishes. Here, an electrode becomes thick if the condition  $\Delta/L_d^0 > 1.6$  is obeyed. Then,  $\tanh(\Delta/L_d^0)$  in expression (25) reaches a maximum possible value of unity, and the net current density stops depending on an increase in the GPE thickness. For a GPE to become thin, the condition  $\Delta/L_d^0 \ll 1$  must be fulfilled. Then,  $\tanh(\Delta/L_d^0)$  in expression (25) can be considered as approximately equal to  $\Delta/L_d^0$ , and the magnitude of the net current density becomes directly proportional to the GPE thickness.

For a further analysis of processes in GPE, it is worthwhile to determine the effective depth  $\delta$  to which the electrochemical gas-generation process penetrates in GPE. We assume that, until the effective depth is reached, the current density (the amount of gas generated in a unit volume of GPE) is constant and equal to a maximum possible current density. The latter follows from (1) in which the oversaturation  $\bar{c}$  is taken to equal unity. In other words, we assume that, in the region of dimensions  $\delta$  that is equivalent to the true variable distribution of current density in GPE, to a distribution that extends to thicknesses greater than  $\delta$ ,

$$j \equiv j_{\max} = i_0 (e^{\beta\eta} - e^{-\alpha\eta}). \quad (27)$$

Then, the effective size of a gas-generation region will be defined by the obvious expression

$$I = j_{\max} \delta S. \quad (28)$$

For  $I$  in (28), we may substitute expression (25). Then,

$$\delta/L_d^0 = e^{-\alpha\eta/2} \{ e^{(\alpha+\beta)\eta} - [\varphi e^{(\alpha/2+\beta)\eta} \tanh(\Delta e^{-\alpha\eta/2}/L_d^0) + 1] / [\varphi e^{-\alpha\eta/2} \tanh(\Delta e^{-\alpha\eta/2}/L_d^0) + 1] \} \times \tanh(\Delta e^{-\alpha\eta/2}/L_d^0) / (e^{\beta\eta} - e^{-\alpha\eta}). \quad (29)$$

#### 4. PARTIAL CASES

One of the two cases that are of special practical interest for the electrochemical gas generation in GPE is the production of hydrogen from water using platinum-group catalysts. The other is the production of chlorine from a NaCl solution on dimensionally stable anodes (DSA).

##### *Production of Hydrogen on Platinum*

As shown, say, in monograph [8], in this case, the transfer coefficients in all the above expressions may be true coefficients. Suppose, for definiteness sake, that  $\alpha = \beta = 0.5$ . Then, instead of (25), we obtain

$$I = I_d e^{-(\eta/4)} (e^\eta - [\varphi e^{(3/4)\eta} \tanh(\Delta e^{-(\eta/4)}/L_d^0) + 1] / [\varphi e^{-(\eta/4)} \tanh(\Delta e^{-(\eta/4)}/L_d^0) + 1]) \tanh(\Delta e^{-(\eta/4)}/L_d^0). \quad (30)$$

The Tafel region of a polarization curve has the form

$$I = I_d e^{\eta/2} (\Delta/L_d^0). \quad (31)$$

The oversaturation on the front surface of GPE is

$$\bar{c}_s = [\varphi e^{(3/4)\eta} \tanh(\Delta e^{-(\eta/4)}/L_d^0) + 1] / [\varphi e^{-(\eta/4)} \tanh(\Delta e^{-(\eta/4)}/L_d^0) + 1]. \quad (32)$$

The effective depth  $\delta$  to which the electrochemical gas-generation process penetrates in GPE is

$$\begin{aligned} \delta/L_d^0 = & e^{-(\eta/4)} \{ e^\eta - [\varphi e^{(3/4)\eta} \tanh(\Delta e^{-(\eta/4)}/L_d^0) \\ & + 1] / [\varphi e^{-(\eta/4)} \tanh(\Delta e^{-(\eta/4)}/L_d^0) + 1] \} / (e^{\eta/2} - e^{-\eta/2}). \end{aligned} \quad (33)$$

#### Production of Chlorine on DSA

In this case, the transfer coefficients in all the expressions of Sections 1–3 must be viewed as apparent coefficients, and it should be assumed that  $\alpha = 0$ ,  $\beta = 2$ . Then, instead of (25), we obtain

$$\begin{aligned} I = I_d(e^{2\eta} - [\varphi e^{2\eta} \tanh(\Delta/L_d^0) \\ + 1] / [\varphi \tanh(\Delta/L_d^0) + 1]) \tanh(\Delta/L_d^0). \end{aligned} \quad (34)$$

The Tafel region of a polarization curve has the form

$$I = I_d e^{2\eta} \tanh(\Delta/L_d^0) / [\varphi \tanh(\Delta/L_d^0) + 1]. \quad (35)$$

If  $\varphi = 0$  (no limitations in the outside-electrode space), the net current density reaches the maximum possible value

$$I = I_{\max} = I_d(e^{2\eta} - 1) \tanh(\Delta/L_d^0). \quad (36)$$

If  $\varphi \tanh(\Delta/L_d^0) \gg 1$ , the net current density stops depending on the GPE thickness. Then,

$$I = I_d(e^{2\eta} - 1)/\varphi, \quad (37)$$

$$\bar{c}_s = [\varphi e^{2\eta} \tanh(\Delta/L_d^0) + 1] / [\varphi \tanh(\Delta/L_d^0) + 1], \quad (38)$$

$$\delta/L_d^0 = \tanh(\Delta/L_d^0) / [\varphi \tanh(\Delta/L_d^0) + 1]. \quad (39)$$

For a virtually infinitely thick DSA, if the condition  $\Delta > 1.6L_d^0$  is obeyed,  $\tanh(\Delta/L_d^0)$  becomes identical to unity. Then, instead of (34), we obtain

$$I = I_d(e^{2\eta} - 1)/(\varphi + 1). \quad (40)$$

In this case,

$$I = I_d e^{2\eta} / (\varphi + 1), \quad (41)$$

$$\bar{c}_s = [\varphi e^{2\eta} + 1] / [\varphi + 1], \quad (42)$$

$$\delta = L_d^0 / [\varphi + 1]. \quad (43)$$

The last quantity stops depending on the overvoltage as well.

For a virtually thin DSA, if the condition  $\Delta \ll L_d^0$ ,  $\tanh(\Delta/L_d^0)$  in expressions (34)–(36) can be replaced with  $\Delta/L_d^0$ . In this case, the net current density linearly depends on the DSA thickness.

## 5. GAS-GENERATION MODES

Basic characteristics of GPE, i.e.,  $I$ ,  $\bar{c}_s$ , and  $\delta$  are defined chiefly by the main parameter  $\varphi$ . Consider two limiting cases,  $\varphi \ll 1$  and  $\varphi \gg 1$ .

Let  $\varphi \ll 1$ . Formally, this occurs when  $\psi \rightarrow \infty$ . The implication is that the characteristic diffusion current in GPE,  $I_d$ , is much less than that in the electrolyte chamber,  $I_g$ . As a result, the limitations in the outside-electrode space are completely removed. Then, as follows from (23),

$$\bar{c}_s \equiv 1. \quad (44)$$

The oversaturation of electrolyte with gas on the front surface of GPE takes on a minimum possible value. According to (25),

$$I = I_d e^{-\alpha\eta/2} (e^{(\alpha+\beta)\eta} - 1) \tanh(\Delta e^{-\alpha\eta/2}/L_d^0). \quad (45)$$

$$\begin{aligned} \delta/L_d^0 \\ = e^{-\alpha\eta/2} (e^{(\alpha+\beta)\eta} - 1) \tanh(\Delta e^{-\alpha\eta/2}/L_d^0) / (e^{\beta\eta} - e^{-\alpha\eta}). \end{aligned} \quad (46)$$

Note an important difference between the production of hydrogen on GPE with platinum and the production of chlorine on DSA. In the former case, as for all electrochemical reactions where  $\alpha \neq 0$ , with the overvoltage  $\eta$  tending to infinity,  $\delta$  tends to extend to the entire GPE thickness, no matter how great the thickness. Let us repeat this important conclusion: if  $\alpha \neq 0$  and  $\eta \rightarrow \infty$ , then

$$\delta = \Delta. \quad (47)$$

Only in the case where  $\alpha = 0$ , in particular, during the chlorine production on DSA, at  $\eta \rightarrow \infty$ , the effective penetration depth cannot extend to distances greater than the characteristic diffusion length of GPE. Or, more accurately,

$$\delta = L_d^0 \tanh(\Delta/L_d^0). \quad (48)$$

Only when  $\tanh(\Delta/L_d^0) = 1$ ,  $\delta = L_d^0$ . This occurs at  $\Delta/L_d^0 \geq 1.6$ .

Now, let  $\varphi \gg 1$ . Formally, this occurs when  $Si_0 \rightarrow \infty$ . This means that  $I_d \gg I_g$ . In this case, limitations in the outside-electrode space play the crucial role. Then, as follows from (23),

$$\bar{c}_s \equiv e^{(\alpha+\beta)\eta}. \quad (49)$$

The oversaturation of electrolyte with gas on the front surface of GPE takes on a maximum value. According to (26),

$$I = I_g (e^{(\alpha+\beta)\eta} - 1). \quad (50)$$

Now, with  $\eta \rightarrow \infty$ ,  $\delta \rightarrow 0$ . This means that the gas-generation process in GPE is forced onto its front sur-

face. Let us find out how  $\delta$  decreases with  $\phi$  tending to infinity. This dependence has the general form

$$\delta = (L_d^0/\phi)(e^{(\alpha+\beta)\eta} - 1)/(e^{\beta\eta} - e^{-\alpha\eta}). \quad (51)$$

In a partial case of the chlorine generation on DSA, at  $\alpha = 0$ ,

$$\delta = L_d^0/\phi. \quad (52)$$

## 6. EXPERIMENTAL FACTS

Consider experimental facts obtained when studying particular GPE. As an example, we will consider two practically important cases, i.e. GPE used for the production of gaseous hydrogen [9–14] and chlorine [15–20]. We will focus on two instances.

(1) The important feature that calls for theoretical explanation is the presence of a special region in the polarization curves for the evolution of hydrogen [13, 14] and chlorine. The authors of [15] called this region the "low-polarizability region." The research on this issue was finalized in review [20]. This is the polarization-curve region (following the Tafel portion), where the net current density increases by more than an order of magnitude in a narrow overvoltage range. Several hypotheses were put forth concerning the origin of the low-polarizability region. V.V. Losev [21] attributed the rapid increase in the DSA current to the emergence of a limiting oversaturation of electrolyte with gas near the front surface of the porous electrode. Under these conditions, the gas is removed much easier: largely through the formation of gas bubbles, rather than by means of diffusion of chlorine molecules in electrolyte in the interelectrode space. According to R.G. Erenburg and L.I. Krishtalik [22], at low overvoltages, gas is generated only in a small part of the inner pore space of DSA. They believed that, in the low-polarizability region, this part gradually expanded and finally spread over the entire thickness of a standard-size electrode. The reasons for the expansion were not established. Recently, S.V. Evdokimov [23] has considered chlorine evolution as a self-accelerating process. The assumption was that, once gas bubbles started to evolve, the electrolyte in the pores began moving and a convective term emerged in the equations, which resulted in a sharp current increase. Sadly, no attempt was undertaken to theoretically substantiate the possibility of the electrolyte motion.

We can explain the origin of the low-polarizability region as follows. The substantial increase in the net current density in DSA is due to a virtually complete elimination of limitations in the outside-electrode space. This is exactly what happens in reality when the overvoltage in a polarization curve for the hydrogen or chlorine evolution reaches a critical value indicating the emergence of first gas pores in the electrode. In the low-polarizability region, the number of gas pores starts to rapidly increase. Finally, trains of gas pores

emerge that are connected with each other and with the front surface of the electrode. In this manner, a powerful channel is created for collecting, in the porous electrode, the gas from the electrolyte pores (on whose inner surface the gas-generation process occurs) and for removing it into the outside-electrode space. The channel is capable of conducting hundreds of amperes per  $\text{cm}^2$  away from the electrode without any losses. Under these conditions, there is no need for chlorine molecules dissolved in electrolyte to reach the front surface via diffusion and then reach the gas-collecting chamber, also via diffusion and agglomeration of gas molecules into gas bubbles. In the low-polarizability region, gas bubbles, avoiding the inner-electrode and outside-electrode diffusion processes, are now capable of directly entering the electrolyte chamber from mouths of gas pores that emerge on the front surface of GPE.

(2) The other fact still not explained theoretically is the severe outside-electrode limitations discovered when studying the chlorine evolution on DSA [15, 16]. According to experimental dependences, in weakly-acidic chloride solutions at  $80^\circ\text{C}$ , under conditions approaching those in industrial production of chlorine, the latter evolves under diffusion control. That the process is controlled by the diffusion removal of chlorine molecules from the front surface of GPE was convincingly demonstrated by experiments on the rotating disk GPE. With increasing electrode rotation rate, the anodic chlorine evolution accelerated. To make quantitative estimates (see next section), it is necessary to estimate the characteristic diffusion length  $L_d^0$ , which enters theoretical expressions and is defined by expression (3). When estimating, we assume that, in equations (3), (9), and (11),  $n = 2$ ; the liquid porosity of DSA  $g_1 = 0.5$ ; the diffusion coefficient for chlorine in electrolyte  $D = 10^{-5} \text{ cm}^2 \text{ s}^{-1}$ ; the chlorine solubility in electrolyte (high NaCl concentrations,  $80^\circ\text{C}$ )  $c_0 = 2.7 \times 10^{-6} \text{ mol cm}^{-3}$ ; the specific surface area of pores in DSA  $S = f/\Delta = 700/510^{-4} = 1.4 \times 10^6 \text{ cm}^{-1}$ , where  $f$  is the roughness factor and  $\Delta$  is the standard thickness of DSA;  $i_0 = 1.2 \times 10^{-4} \text{ A cm}^{-2}$  [24]; and  $F = 10^5 \text{ C mol}^{-1}$ . We also assume that  $\nu = 1$  in expression (4) for the effective diffusion coefficient. Then, for a DSA of standard thickness  $\Delta = 5 \text{ }\mu\text{m}$ , we obtain  $L_d^0 = 1.27 \text{ }\mu\text{m}$ ,  $I_d = 21 \text{ mA cm}^{-2}$ , and  $I_k = i_0 S \Delta = 84 \text{ mA cm}^{-2}$ .

## 7. THEORETICAL ESTIMATES

As we mentioned in the foregoing, the severe outside-electrode limitations that were experimentally observed on DSA must be observed in the case where  $\phi \gg 1$  in GPE. Sadly, it is not easy to estimate parameter  $\phi$ , because the value of parameter  $\psi$  in definition (26) is unknown. Parameter  $\psi$  defines the formation rate of gas bubbles in the electrolyte chamber, as is seen from (17). And yet, parameters  $\phi$  and  $\psi$  may be esti-

**Table 1.** The dependence of the  $I_{\Delta=5}/I_{\Delta=0.2}$  ratio as a function of parameter  $\varphi$ 

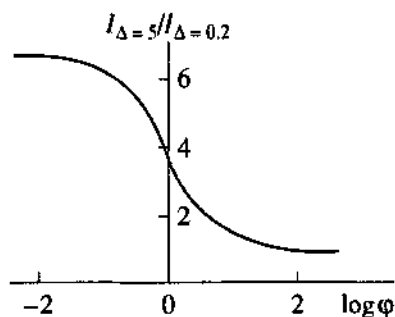
$\varphi$	0.0	0.2	0.5	1	10	100	$\infty$
$I_{\Delta=5}/I_{\Delta=0.2}$	6.67	5.72	4.78	3.83	1.52	1.06	1.0

**Table 2.** The absolute and reduced penetration depths of the chlorine-generation process in DSA of standard 5  $\mu\text{m}$  thickness as a function of  $\varphi$ 

$\varphi$	0	0.1	1	5	10	50	100	$\infty$
$\delta/L_d^0$	1.0	0.9	0.5	0.17	0.09	0.02	0.01	0
$\delta, \mu\text{m}$	1.27	1.15	0.635	0.21	0.12	0.025	0.013	0

mated by experimentally comparing current densities for thick and thin GPE in the Tafel portions of polarization curves. We will vary the main parameter of the system under study,  $\varphi$ . In the first place, let us perform selective estimates. The dependence of the ratio of current densities in DSA 5 and 0.2  $\mu\text{m}$  thick,  $I_{\Delta=5}/I_{\Delta=0.2}$ , on parameter  $\varphi$  is calculated with (35). The dependences of the absolute ( $\delta$ ) and reduced ( $\Delta/L_d^0$ ) effective penetration depths of the process of the electrochemical chlorine generation into the pore space of a DSA of standard thickness, for which  $\Delta/L_d^0 = 5/1.27 = 3.94$ , are calculated with (39). The results are presented in Tables 1 and 2.

The entire  $I_{\Delta=5}/I_{\Delta=0.2}$  vs.  $\log\varphi$  dependence is presented in Fig. 1. Parameter  $\varphi$  may be considered equal to almost zero starting with  $\varphi = 0.01$ , when the  $I_{\Delta=5}/I_{\Delta=0.2}$  ratio reaches its maximum value of  $1/0.15 = 6.67$ . And parameter  $\varphi$  may be considered equal to almost infinity starting with  $\varphi = 100$ , when the  $I_{\Delta=5}/I_{\Delta=0.2}$  ratio reaches its minimum value of unity. The dependence of  $\delta/L_d^0$  on  $\log\varphi$  is presented in Fig. 2 for some DSA thicknesses. Again we see that  $\varphi$  is virtually zero at  $\varphi = 0.01$  and is virtually infinitely large at  $\varphi = 100$ . In the chlorine production, DSA may be considered infinitely thick if its thickness exceeds 1.6 times 1.27  $\mu\text{m}$  which makes 2.03  $\mu\text{m}$ ; then we can take

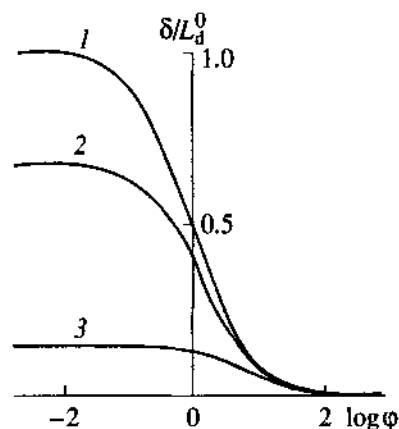
**Fig. 1.** The  $I_{\Delta=5}/I_{\Delta=0.2}$  ratio as a function of  $\varphi$ .

$\tanh(\Delta/L_d^0) = 1$ . Thus, it appears that DSA of the standard thickness 5  $\mu\text{m}$  may be viewed as an infinitely thick electrode. With such an electrode, even at very small  $\varphi$  (Fig. 2, curve 1), the gas-generation process penetrates to a maximum possible depth  $\delta = L_d^0 = 1.27 \mu\text{m}$ , provided all limitations in the outside-electrode space are removed. This value of  $\delta$  is lower than the DSA thickness by approximately four times. With the DSA thickness diminished (Fig. 2, curves 2, 3),  $\delta$  becomes even smaller. At high  $\varphi$ , on the other hand, the right-hand branches of curves 1–3 in Fig. 2 converge. Here,  $\delta$  drops to zero with increasing  $\varphi$  in DSA of any thickness: the process is forced out, onto the front surface of DSA, because the outside-electrode limitations, rather than the DSA characteristics, become the determining factor at these values of  $\varphi$ .

Figure 3 shows how the oversaturation of electrolyte with gas on the front surface of DSA depends on  $\log\varphi$ . The dependences were calculated for DSA of the standard thickness 5  $\mu\text{m}$  at overvoltages  $\eta$  of 0.5 and 1.0. As seen, in the region of low  $\varphi$ , where the limitations in the outside-electrode space are presumably eliminated altogether, the oversaturation reaches its minimum possible value of unity. However, with increasing  $\varphi$ , the outside-electrode limitations start to play an ever more perceptible role. At  $\varphi \geq 100$ , the oversaturation reaches the maximum possible value at a given  $\eta$ , specifically,

$$(\bar{c}_s)_{\max} = e^{2\eta}. \quad (53)$$

Up to this point, we have paid no attention to characteristics of processes proceeding in the electrolyte chamber. The main parameter of this region is the proportionality coefficient  $\psi$  in expression (17). As the sequence of processes leading to the final result, i.e. to the formation of gas bubbles in the electrolyte chamber and their removal from it, is very complex, parameter  $\psi$  cannot be estimated directly. Hence, let us try to estimate it indirectly. Consider Table 1. Suppose that the

**Fig. 2.** The  $\delta/L_d^0$  vs.  $\varphi$  dependences for  $\Delta$  of (1) 5, (2) 1, and (3) 0.2  $\mu\text{m}$ .

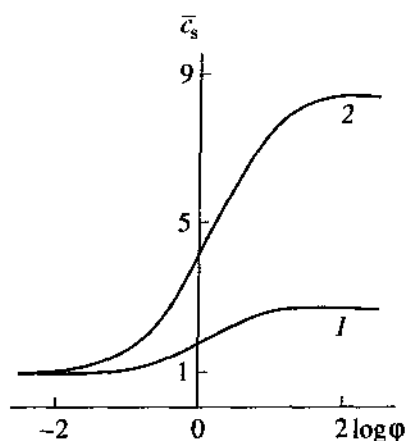


Fig. 3. The  $\bar{c}_s$  vs.  $\phi$  dependence for the gaseous chlorine generation in DSA  $5 \mu\text{m}$  thick at  $\eta$  of (1) 0.5 and (2) 1.

$I_{\Delta=5}/I_{\Delta=0.2}$  ratio was found experimentally on DSA. Obviously, it is not necessary for a thin electrode to be  $0.2 \mu\text{m}$  thick. Once we have determined this ratio, the magnitude of parameter  $\phi$  is determined as well, as follows from Table 1 and Fig. 1. But we can then get busy with a numerical estimation of parameter  $\psi$  and all quantities that depend on it and characterize processes in the electrolyte chamber. Suppose, for definiteness sake, that the experimental  $I_{\Delta=5}/I_{\Delta=0.2}$  ratio is equal to 1.52. In accordance with Table 1,  $\phi = 10$ . Employing relationship (24), then

$$\psi = Si_0 g_l / nFV\phi^2 = 4.210^{-6} \text{ mol cm}^{-3} \text{ s}^{-1}, \quad (54)$$

and the characteristic flow of removal of chlorine molecules in a unit volume of the electrolyte chamber from a state of dissolved molecules directly into a gas phase (bubbles of chlorine gas leaving the electrolyte chamber) is

$$nF\psi = 8.4 \times 10^{-1} \text{ A cm}^{-3}. \quad (55)$$

It is useful to compare this quantity with the amount of current generated by a unit porous volume in DSA, specifically,  $Si_0 = 168 \text{ A cm}^{-3}$ . As seen, the gas-generation intensity in DSA pores is 200 times the chlorine removal intensity in the electrolyte chamber. Relationship (19) allows us to estimate the characteristic diffusion length for the electrolyte chamber,  $L_r = (Dc_0/\psi)^{1/2} = 25.4 \mu\text{m}$ . Hence, for a full-capacity operation of the electrolyte chamber, to ensure the removal of chlorine generated in DSA, the chamber's width must be approximately  $30 \mu\text{m}$ . It is useful to compare  $L_r$  with the characteristic diffusion length for porous space of

DSA,  $L_r = 1.27 \mu\text{m}$  (see above). Finally, using (23), we can compare the characteristic diffusion current in the electrolyte chamber,  $I_r = nF(Dc_0\psi)^{1/2} = 2.1 \text{ mA cm}^{-2}$ , with that in GPE,  $I_d = 21 \text{ mA cm}^{-2}$ . As expected, the currents differ by an order of magnitude.

## REFERENCES

1. Chirkov, Yu.G., *Elektrokhimiya*, 1971, vol. 7, p. 1512.
2. Chirkov, Yu.G., *Elektrokhimiya*, 1971, vol. 7, p. 1681.
3. Chirkov, Yu.G. and Pshenichnikov, A.G., *Elektrokhimiya*, 1984, vol. 20, p. 1542.
4. Chirkov, Yu.G. and Pshenichnikov, A.G., *Itogi Nauki Tekh., Ser.: Elektrokhimiya*, 1988, vol. 27, p. 199.
5. Chirkov, Yu.G. and Pshenichnikov, A.G., *Elektrokhimiya*, 1994, vol. 30, p. 1338.
6. Chirkov, Yu.G. and Rostokin, V.I., *Elektrokhimiya*, 1996, vol. 32, p. 1082.
7. Chirkov, Yu.G. and Pshenichnikov, A.G., *Elektrokhimiya*, 1997, vol. 33, p. 956.
8. Vetter, K.J., *Elektrochemische Kinetik*, Berlin: Springer, 1961.
9. Heidrich, G.-Y., Podlovchenko, B.I., and Muller, L., *Elektrokhimiya*, 1988, vol. 24, p. 1119.
10. Muller, L., Heidrich, G.-Y., and Podlovchenko, B., *J. Appl. Electrochem.*, 1990, vol. 20, p. 686.
11. Podlovchenko, B.I., Maksimov, Yu.M., Heidrich, G.-Y., et al., *Elektrokhimiya*, 1991, vol. 27, p. 864.
12. Muller, L. and Heidrich, G.-Y., *Elektrokhimiya*, 1989, vol. 25, p. 1145.
13. Schonfuss, D. and Muller, L., *Electrochim. Acta*, 1994, vol. 39, p. 2097.
14. Schonfuss, D., Spitzer, H.-J., and Muller, L., *Elektrokhimiya*, 1995, vol. 31, p. 1008.
15. Pecherskii, M.M., Gorodetskii, V.V., Evdokimov, S.V., and Losev, V.V., *Elektrokhimiya*, 1981, vol. 17, p. 1087.
16. Evdokimov, S.V., Gorodetskii, V.V., and Losev, V.V., *Elektrokhimiya*, 1985, vol. 21, p. 1427.
17. Evdokimov, S.V. and Gorodetskii, V.V., *Elektrokhimiya*, 1986, vol. 22, p. 782.
18. Evdokimov, S.V. and Gorodetskii, V.V., *Elektrokhimiya*, 1986, vol. 22, p. 982.
19. Evdokimov, S.V. and Gorodetskii, V.V., *Elektrokhimiya*, 1989, vol. 25, p. 1139.
20. Gorodetskii, V.V., Evdokimov, S.V., and Kolotykin, Ya.M., *Itogi Nauki Tekh., Ser.: Elektrokhimiya*, 1991, vol. 34, p. 84.
21. Losev, V.V., *Elektrokhimiya*, 1981, vol. 17, p. 733.
22. Erenburg, R.G. and Krishtalik, L.I., *Elektrokhimiya*, 1987, vol. 23, p. 8.
23. Evdokimov, S.V., *Elektrokhimiya*, 1998, vol. 34, p. 979.
24. Evdokimov, S.V., Mishenina, K.A., and Gorodetskii, V.V., *Elektrokhimiya*, 1988, vol. 24, p. 1475.